

Fig. 2 Film cooling effectiveness with injection of refrigerant 12 for $M = 0.0082 - 0.0115$, $T_2 = 328 - 355^\circ\text{K}$ [taking $c_{p2}/c_{p1} = 1.58$, and $Pr_{\infty} = 0.728$ and $Re_2 \mu_2/\mu_{\infty} = 1290$ [used in Eq. (5)]].

present data and provide reasonable agreement with the modified theoretical models of subsonic film cooling. The model of Kutateladze and Leont'ev [Eq. (4)], although not realistic in its assumptions of uniform mixture and temperature across the boundary layer, predicts the experimental data obtained with refrigerant 12 injection excellently (Fig. 2). This model also predicts the air injected data,^{4,10} but fails to predict adequately the data for helium injection. The helium injection data are approximated better by Eq. (5) which had been used to predict subsonic film cooling effectiveness with air and helium injection.³ Shadowgraph observations indicate that the composition of the injected gas affects the boundary-layer thickness. This effect is included in Eq. (5) by the molecular weight ratio in parameter β . Rederiving Eq. (4) to include this effect on boundary-layer thickness gives better agreement with the data for helium injection, but the new equation, besides being complicated, does not adequately predict the results of refrigerant 12 injection.

One can thus conclude that there is relatively good agreement between the experimental data for supersonic film cooling and modified theoretical models of subsonic film cooling when a foreign gas is injected through a porous section into the main flow.

References

- ¹ Kutateladze, S. S. and Leont'ev, A. I., "Film Cooling with a Turbulent Gaseous Boundary Layer," *Thermal Physics of High Temperature*, Vol. 1, No. 2, 1963, pp. 281-290.
- ² Stollery, J. L. and El-Ehway, A. A. M., "A Note on the Use of a Boundary Layer Model for Correlating Film Cooling Data," *International Journal of Heat and Mass Transfer*, Vol. 8, No. 1, Jan. 1965, pp. 55-65.
- ³ Goldstein, R. J. and Haji-Sheikh, A., "Prediction of Film Cooling Effectiveness," *Proceedings of the JSME 1967 Semi-International Symposium*, Vol. 1, 1967, pp. 213-218.
- ⁴ Goldstein, R. J., Eckert, E. R. G., and Wilson, D. J., "Film Cooling with Normal Injection Into a Supersonic Flow," *Transactions of the ASME, Journal of Engineering for Industry*, Vol. 90, Series B, No. 4, Nov. 1968, pp. 584-587.
- ⁵ Goldstein, R. J., Rask, R. B., and Eckert, E. R. G., "Film Cooling with Helium Injection into an Incompressible Air Flow," *International Journal of Heat and Mass Transfer*, Vol. 9, No. 12, Dec. 1966, pp. 1341-1350.
- ⁶ Nishiwaki, N., Hirata, M., and Tsuchida, A., "Heat Transfer on a Surface Covered by a Cold Air Film," *International Developments in Heat Transfer*, International Heat Transfer Conference, 1961, Boulder, Colo., ASME 1961, pp. 675-681.
- ⁷ Goldstein, R. J., Tsou, F. K., and Eckert, E. R. G., "Film Cooling in Supersonic Flow," *Proceedings of Second All-Soviet Union Conference on Heat and Mass Transfer*, Vol. 2, 1967, pp. 226-247.
- ⁸ Goldstein, R. J. et al., "Film Cooling with Air and Helium Injection Through a Rearward Facing Slot into Supersonic Air Flow," *AIAA Journal*, Vol. 4, No. 6, June 1966, pp. 981-985.
- ⁹ Mukerjee, T. and Martin, B. W., "Film Cooling by Air Injection Through a Backward Facing Annular Tangential Slot in a

Supersonic Axisymmetric Parallel Diffuser," *Proceedings of the 1968 Heat Transfer and Fluid Mechanics Institute*, Stanford University Press, 1968, pp. 221-242.

¹⁰ Jabbari, M. Y., "Film Cooling Effectiveness with Normal Injection of Air, Helium, and Freon 12 into a Mach 3 Flow of Air," M.S. Thesis, Univ. of Minnesota, 1969.

Undestructive Determination of the Buckling Load of an Elastic Bar

MENACHEM BARUCH*

Georgia Institute of Technology, Atlanta, Ga.

Introduction

IT was always important to find some practical method of determining the buckling load of a bar without destroying it. The famous Southwell¹ plot is a very important one, but it requires loading in the direction of the bar's axis, and the load must approach the critical value. Another method recently was proposed by Horton and Struble.² In this method the load is applied in a direction perpendicular to the bar's axis. By measuring the deflections or the angles of rotation of the deflected bar, it was found that there is a connection between the buckling load and these two parameters. The method works well in some cases but not so well in other cases, especially when one end is laterally restricted by an elastic spring. In this case the method ceases to be exact enough. The reason why the proposed Horton and Struble method fails in some cases may be as follows. (See Figs. 1 and 2.)

For the two structural systems seen in Figs. 1 and 2, the bars and the springs at the ends are the same, but the boundary conditions are different. When at least one of the two lateral spring constants (β_1, β_2) is zero or finite, the buckling force P enters into the boundary conditions in Fig. 1. Therefore, the respective boundary conditions in the two cases are different. This is probably the reason why the method proposed in Ref. 2 fails when the bar is supported on lateral springs. The Southwell plot works well because the boundary conditions are fulfilled all the time.

The boundary conditions in Figs. 1 and 2 are not the same, but the spring constants ($\alpha_1, \alpha_2, \beta_1, \beta_2$) are identical. Based on this fact, another method which is more general and will work in all the cases in the elastic region is proposed here.³ By loading the bar as in Fig. 2 and measuring deflections and rotations it is possible to obtain data from which to calculate the spring constants and then to calculate the buckling load.



Fig. 1 Spring constrained beam loaded by axial force P .

Received April 9, 1970; revision received July 20, 1970. This research was supported, in part, by the Air Force Office of Scientific Research under Grant AFOSR-68-1476 and by the National Science Foundation. The author would like to thank the National Science Foundation for Foreign Senior Scientists, whose Fellowship gave him the opportunity to spend a year at Georgia Institute of Technology, Atlanta, Ga. The author is grateful to Professor W. H. Horton of the School of Aerospace Engineering, Georgia Institute of Technology for useful discussions and ideas.

* Visiting Professor in the School of Aerospace Engineering, Georgia Institute of Technology, Atlanta, Ga. On leave from Technion, Haifa, Israel. Member AIAA.

Spring Constants for Beam with Constant Stiffness (see Fig. 3)

The measured deflections δ_1 , δ_2 and the measured rotations φ_1 , φ_2 of the supports caused by a load $Q = 1$ (See Fig. 3) are connected with the general deflection v in the following manner

$$\begin{aligned}\varphi_1 &= (dv/dx)_{x=0} & \varphi_2 &= (dv/dz)_{z=0} \\ \delta_1 &= (v)_{x=0} & \delta_2 &= (v)_{z=0}\end{aligned}\quad (1)$$

Using the boundary conditions of Eq. (1) one obtains for $0 \leq x \leq a$

$$\begin{aligned}EI(d^2v/dx^2) &= -M(x) = M_1 - A_1x \\ EI(dv/dx) &= M_1x - A_1(x^2/2) + EI\varphi_1\end{aligned}\quad (2)$$

$$EIv = M_1(x^2/2) - A_1(x^3/6) + EI\varphi_1x + EI\delta_1$$

for $0 \leq z \leq b$

$$\begin{aligned}EI(d^2v/dz^2) &= -M(z) = M_2 - A_2z \\ EI(dv/dz) &= M_2z - A_2(z^2/2) + EI\varphi_2\end{aligned}\quad (3)$$

$$EIv = M_2(z^2/2) - A_2(z^3/6) + EI\varphi_2z + EI\delta_2$$

$$\begin{bmatrix} \alpha_1 k & 0 & \alpha_1 \\ \alpha_2 k \cos kl - EI k^2 \sin kl & 0 & \alpha_2 \\ 0 & P & P \\ -\beta_2 \sin kl & P - \beta_2 l & 0 \end{bmatrix} \begin{bmatrix} B_1 \\ B_2 \\ B_3 \\ B_4 \end{bmatrix} = 0 \quad (12)$$

The equilibrium conditions require

$$A_1 + A_2 = Q, \quad M_1 - A_1a - M_2 + A_2b = 0 \quad (4)$$

The compatibility conditions require

$$(dv/dx)_{x=a} = -(dv/dz)_{z=b}, \quad (v)_{x=a} = (v)_{z=b} \quad (5)$$

From Eqs. (4) and (5) one obtains

$$\begin{bmatrix} 1 & 1 & 0 & 0 \\ a & -b & -1 & 1 \\ \frac{a^2}{2} & \frac{b^2}{2} & -a & -b \\ \frac{a^3}{6} & -\frac{b^3}{6} & -\frac{a^2}{2} & \frac{b^2}{2} \end{bmatrix} \begin{Bmatrix} A_1 \\ A_2 \\ M_1 \\ M_2 \end{Bmatrix} = \begin{Bmatrix} Q = 1 \\ 0 \\ EI(\varphi_1 + \varphi_2) \\ EI(\delta_1 - \delta_2) + EI(\varphi_1a - \varphi_2b) \end{Bmatrix} \quad (6)$$

By changing the value of Q and dividing the measured end rotations and deflections by it, better average evaluations of φ_1 , φ_2 , δ_1 and δ_2 will be obtained for $Q = 1$.

After calculation of the boundary moments and forces, the spring constants must be evaluated by the relations

$$\begin{aligned}\alpha_1 &= M_1/\varphi_1 & \alpha_2 &= M_2/\varphi_2 \\ \beta_1 &= A_1/\delta_1 & \beta_2 &= A_2/\delta_2\end{aligned}\quad (7)$$

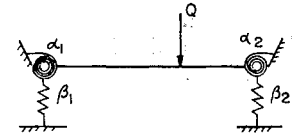
Better statistical values for the spring constants will be obtained by changing the position of Q (a and b).

Buckling Load for Constant Stiffness

The buckling load must be calculated by satisfying the obtained boundary conditions. The stability equation is as usual

$$EI(d^4y/dx^4) + P(d^2y/dx^2) = 0 \quad (8)$$

Fig. 2 Spring constrained beam loaded by lateral force Q .



By defining

$$(P/EI) = k^2 \quad (9)$$

The solution of Eq. (8) will be

$$y = B_1 \sin kx + B_2 x + B_3 \cos kx + B_4 \quad (10)$$

The boundary conditions are

$$\begin{aligned}EI(d^2y/dx^2) - \alpha_1 dy/dx &= 0 \\ EI(d^3y/dx^3) + Pdy/dx + \beta_1 y &= 0\end{aligned}\quad \text{for } x = 0 \quad (11)$$

$$\begin{aligned}EI(d^2y/dx^2) + \alpha_2 dy/dx &= 0 \\ EI(d^3y/dx^3) + Pdy/dx - \beta_2 y &= 0\end{aligned}\quad \text{for } x = l$$

After substitution of Eq. (10) into Eq. (11) one obtains

$$\begin{bmatrix} EI k^2 & 0 & 0 \\ \alpha_2 k \sin kl + EI k^2 \cos kl & 0 & 0 \\ \beta_1 & \beta_1 & \beta_1 \\ -\beta_2 \cos kl & -\beta_2 & -\beta_2 \end{bmatrix} \begin{bmatrix} B_1 \\ B_2 \\ B_3 \\ B_4 \end{bmatrix} = 0 \quad (12)$$

Note that every spring constant appears only in its respective row. When the beam has strong springs it is convenient, before performing the calculations, to divide the row of the strong spring by the high value of the spring constant. In this way calculation difficulties will be avoided. For example, for a beam which behaves nearly like a cantilever clamped at the side $x = l$, it will be convenient to divide the second row of the determinant by α_2 and the fourth row by β_2 before finding the buckling load. The smallest value of P for which the determinant of the matrix becomes zero, is the buckling load appropriate to the real boundary conditions.

For cases where the initial stresses in the bar are in the plastic region it is possible to apply some of the plastic theories for buckling, using the fact that the elastic buckling load is known.

The spring constants of a beam with varying stiffness can be found in a way similar to that proposed for a beam with constant stiffness. For details see Ref. 3.

Conclusion

An undestructive method in which the buckling load of a bar is obtained by determining the actual boundary conditions was described. The spring constants, which represent

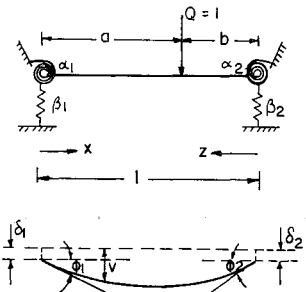
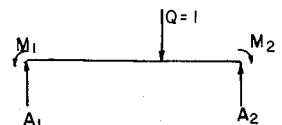


Fig. 3 Deflections, rotations and reactions of a spring constrained beam loaded by a lateral force $Q = 1$.



the boundary conditions, are obtained from measurements of the end deflections and rotations of the bar caused by a lateral load.

References

¹ Southwell, R. V., "On the Analysis of Experimental Observations in Problems of Elastic Stability," *Proceeding of the Royal Society, A*, Vol. 135, 1932, pp. 601-616.

² Horton, W. H. and Struble, D. E., "Non-Destructive Test Techniques in the Prediction of the Buckling Load of a Column," Presented at the 13th Annual Israel Conference on Aviation and Astronautics, Tel Aviv-Haifa, 1970, to be published in the *Israel Journal of Technology*.

³ Baruch, M., "On Undestructive Determination of the Buckling Load of an Elastic Bar," GITAER 70-1, March 1970, School of Aerospace Engineering, Georgia Institute of Technology, Atlanta, Ga.

Axisymmetric Dynamic Buckling of Clamped Shallow Spherical and Conical Shells under Step Loads

NURI AKKAS* AND NELSON R. BAULD JR.†
Clemson University, Clemson, S. C.

THE purpose of this short Note is to present some additional numerical results of the axisymmetric dynamic buckling of clamped shallow spherical shells under step loads of infinite duration and to present, for the first time, similar numerical results for clamped shallow conical shells under the same type of loads.

It is shown that when the critical axisymmetric dynamic buckling loads for the clamped shallow spherical shell are obtained for certain discrete values of the geometric parameter λ , for which this information had not been obtained previously, the axisymmetric dynamic buckling curve (p_D vs λ) is modified in such a way that a striking similarity between the axisymmetric dynamic and the axisymmetric static (p_s vs λ) buckling curves becomes apparent. Indeed, it is shown that a two-dimensional translation of the axisymmetric dynamic buckling curve brings it into good agreement with the axisymmetric static buckling curve for a significant range of the geometric parameter λ .

Similar, and even more striking, results are observed between the axisymmetric dynamic and static buckling curves for the clamped conical shell under the same type of load.

The system of differential equations that govern the nonlinear axisymmetric oscillations of clamped shallow spherical

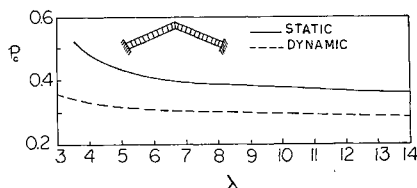


Fig. 1 Axisymmetric static and dynamic buckling behavior of shallow clamped conical caps under uniform pressure.

Received August 7, 1970. The financial support for this investigation was provided by the Department of Engineering Mechanics of Clemson University.

* Research Assistant, Engineering Mechanics Department.

† Professor, Engineering Mechanics Department.

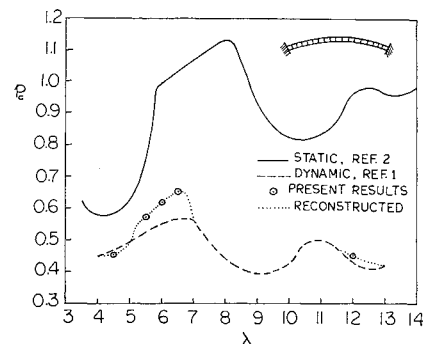


Fig. 2 Axisymmetric static and dynamic buckling behavior of shallow clamped spherical caps under uniform pressure.

and conical shells under step loads of infinite duration can be written in the nondimensional forms

$$\nabla^4 w = g_1 + (1/x) (\Phi w')' + 4p - \ddot{w} \quad (1)$$

$$(x\Phi')' - (1/x)\Phi + g_2 = -\frac{1}{2}(w')^2 \quad (2)$$

where

$$g_1 = \begin{cases} (1/x)(x\Phi)' & \text{for the spherical shell} \\ (\lambda/2x)\Phi' & \text{for the conical shell} \end{cases} \quad (3)$$

$$g_2 = \begin{cases} xw' & \text{for the spherical shell} \\ (\lambda/2)w' & \text{for the conical shell} \end{cases}$$

and

$$\nabla^2 \equiv ()'' + (1/x)()' \quad (4)$$

Primes and dots over quantities signify differentiation with respect to the nondimensional base-plane radius x and the nondimensional time τ . Finally w and Φ are nondimensional transverse displacement and stress functions, respectively, and p is the nondimensional load parameter.

The boundary and initial conditions for both the clamped shallow spherical and conical caps under step loads of infinite duration are the same as those given in Ref. 1 for the clamped shallow spherical shell. Moreover, the numerical procedure described in Ref. 1 is used in the present study. In order to begin the numerical computations for the clamped shallow conical shell, the function $g_1(x=0)$ is assumed to be the same as $g_1(x=0)$ for the clamped shallow spherical shell. This is consistent with the assumption that a spherical inclusion exists in the vicinity of the apex of the conical cap.⁴ Axisymmetric static buckling behavior of the clamped shallow conical shell is analyzed also by discarding the inertia term in Eq. (1).

The axisymmetric static and dynamic buckling curves for the clamped shallow conical shell are shown in Fig. 1 and the corresponding numerical data from which the curves were

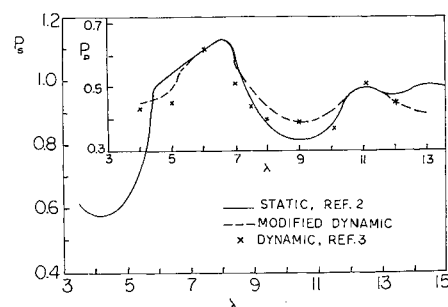


Fig. 3 Comparison of axisymmetric static and dynamic buckling curves of shallow spherical caps under uniform pressure.